Table 8.10: **Oblique analyses with equivelent elastic surface beams**

Analysis	Description
OEB	Properties given in tables 8.3 and 8.4
OEB2	As for OEB but with $EI_{in} \times 10$
OEB3	As for OEB but with $EI_{in} \times 1/5$
OEB4	As for OEB but with $EI_{in} \times 1/10$
OEB5	As for OEB but with $EI_{in} \times 1/100$
OEB6	As for OEB but with $EI_{in} \times 1/1000$

rigid than the front. This observation confirms those of Chapters 5 and 6 where masonry walls in hogging were observed to crack and lose their stiffness, thus suffering greater bending curvatures in soil-structure interaction situations than walls in sagging, which through arching, tend to suffer less curvature. This also concurs with the conclusions drawn by Liu (1997), Augarde (1997) and Burd et al. (2000) for analysis of the same problem.

The north end wall is entirely in the sagging region and, as expected, does not exhibit any significant curvature, although it tilts significantly in a rigid fashion (figure 8.34(c)). The south end wall is mostly outside the region of significant influence of the tunnelling (although there is a slight hogging section, see figure 8.34(d)). It does, however, tilt in a rigid fashion and settle approximately 6mm more than the greenfield profile.

8.3.4 Analysis with equivalent elastic surface beams

Following description of the initial run in this section (OEB) which has elastic surface beams representing the building with properties as given in tables 8.3 and 8.4, a range of analyses are used to investigate the effect of differing in-plane bending stiffness assigned to the beams. The analyses described in this section are summarised in table 8.10.

Equivalent elastic surface beams

Surface displacement results from run type OEB with the building represented by elastic beams are presented in figures 8.35 to 8.37.

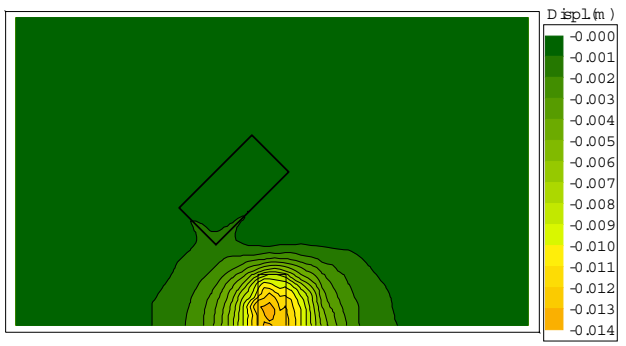

(a) Tunnelling Stage 1

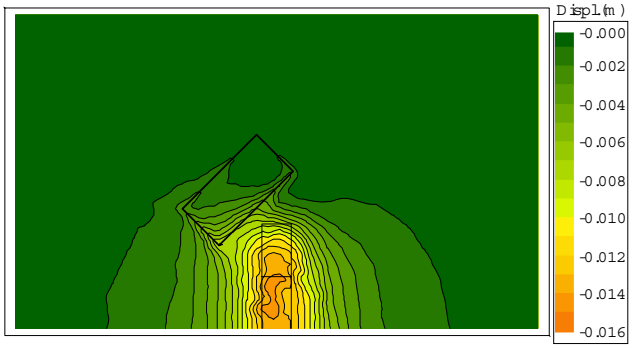

(b) Tunnelling Stage 2

(c) Tunnelling Stage 3

(d) Tunnelling Stage 4

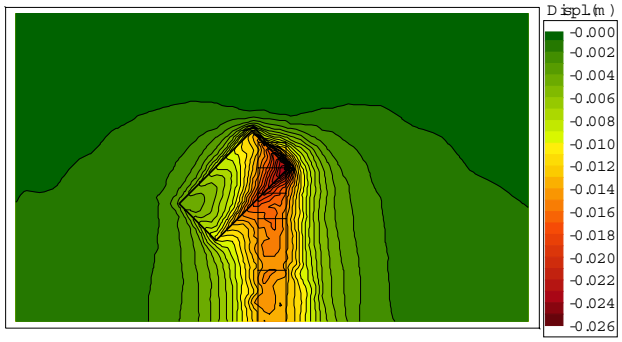

(e) Tunnelling Stage 5

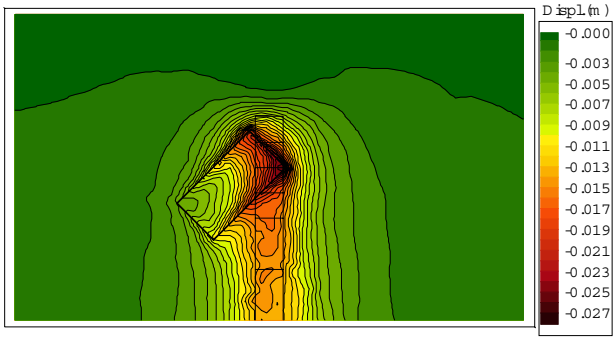

(f) Tunnelling Stage 6

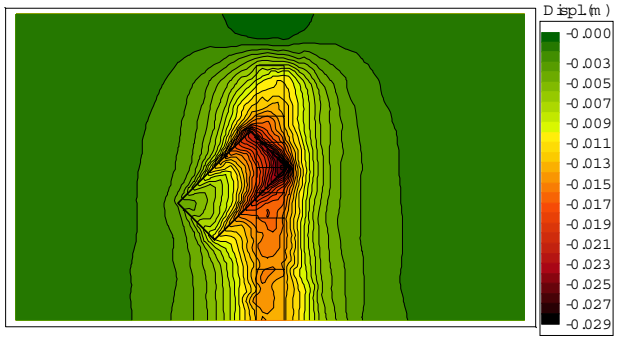

(g) Tunnelling Stage 7

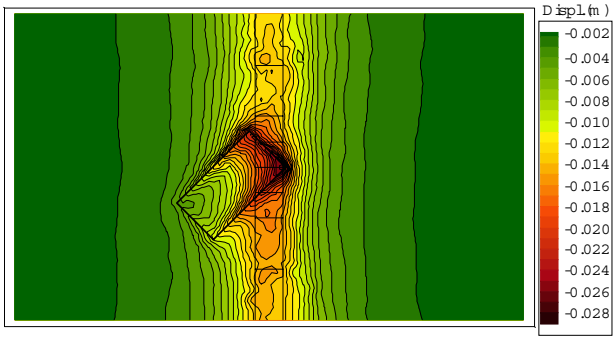

(h) Tunnelling Stage 8

Figure 8.35: **Equivalent elastic surface beams OEB: Surface displacement contours**

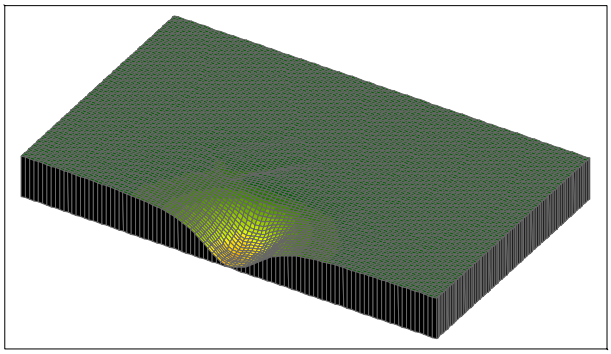

(a) Tunnelling Stage 1

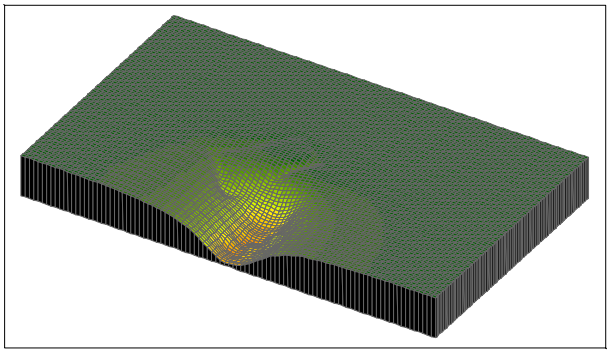

(b) Tunnelling Stage 2

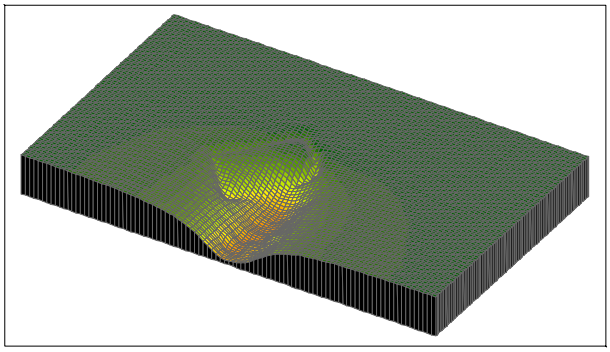

(c) Tunnelling Stage 3

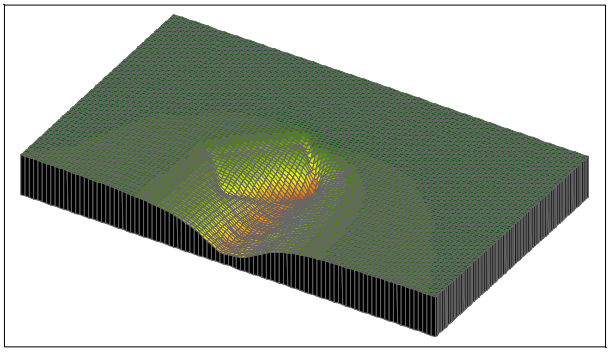

(d) Tunnelling Stage 4

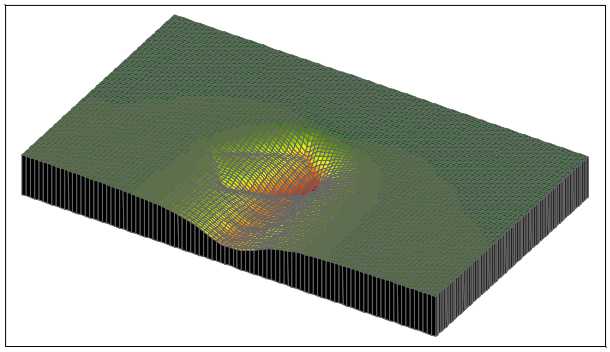

(e) Tunnelling Stage 5

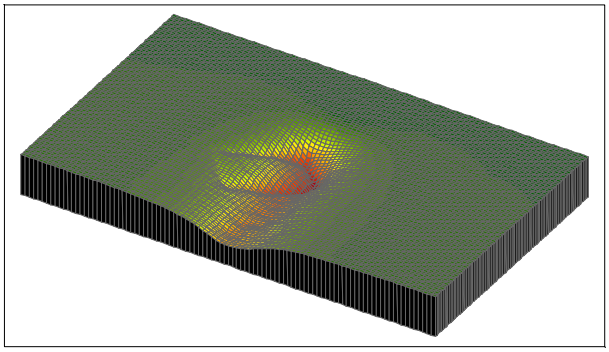

(f) Tunnelling Stage 6

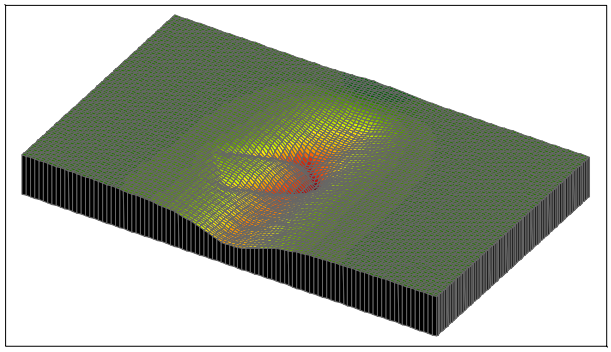

(g) Tunnelling Stage 7

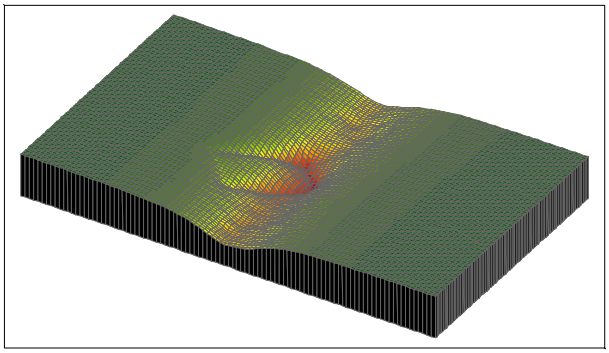

(h) Tunnelling Stage 8

Figure 8.36: **Equivalent elastic surface beams OEB: 3D Surface profile**

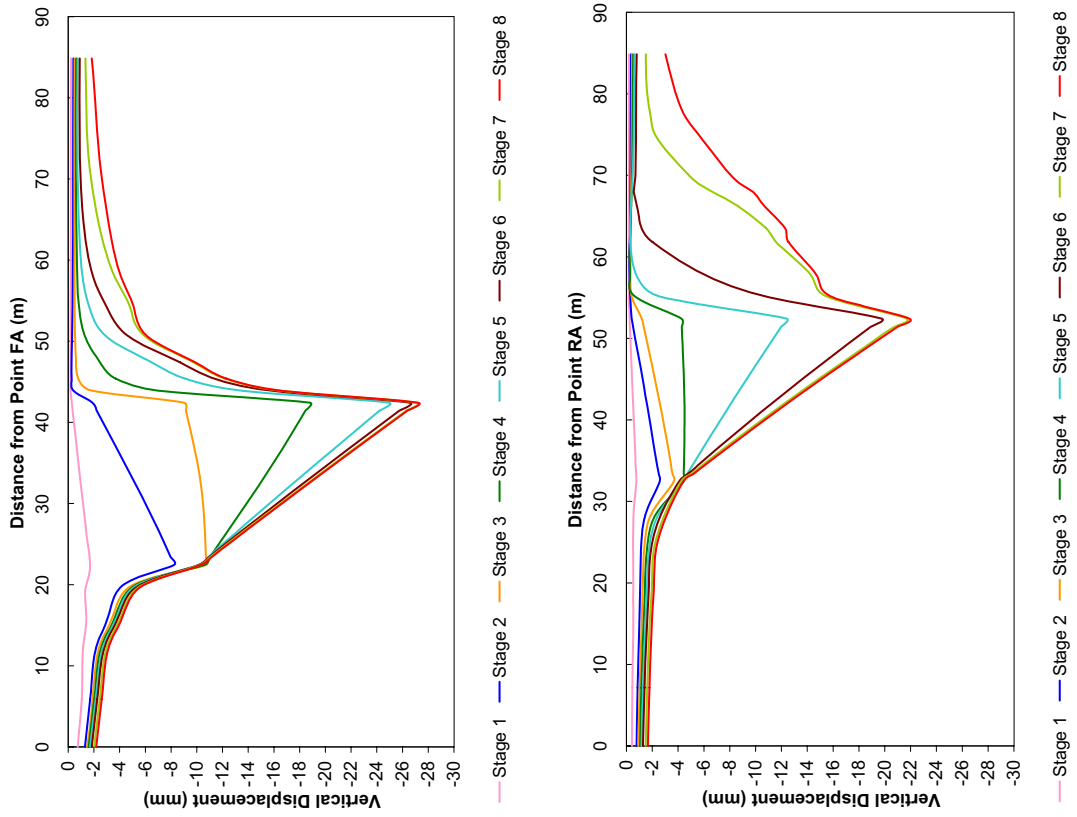

(a) Front facade

(b) Rear facade

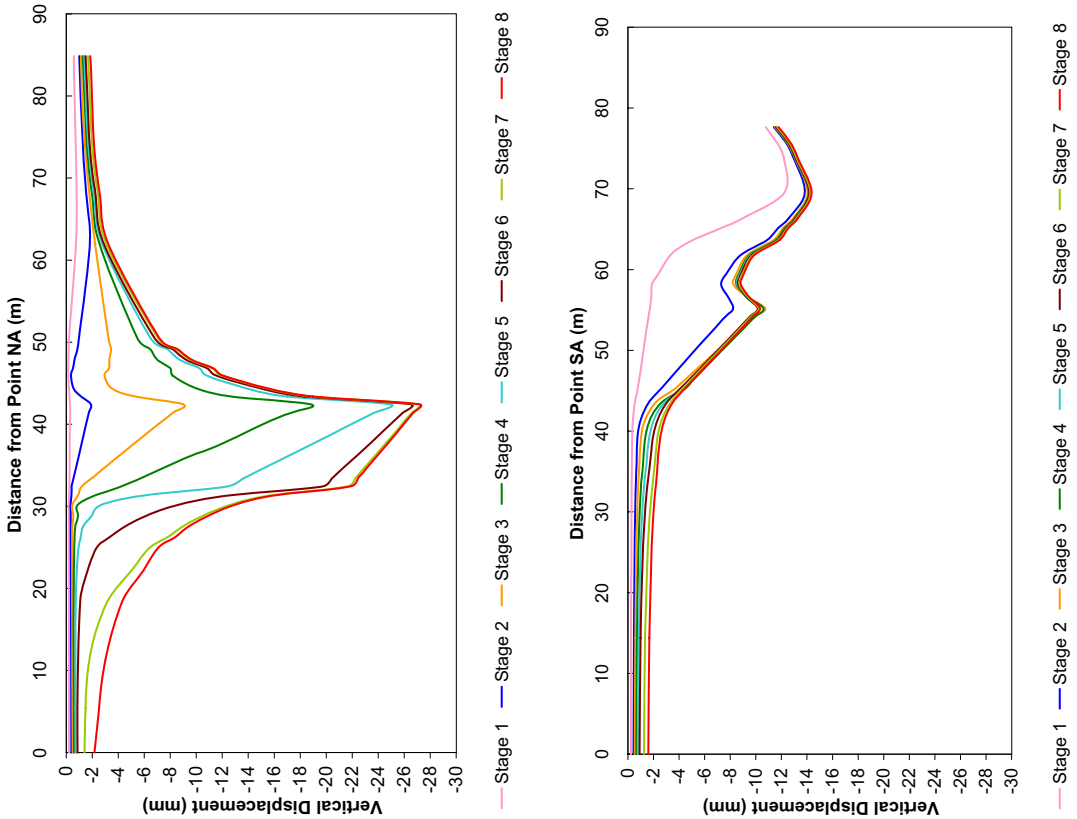

(c) North end wall

(d) South end wall

Figure 8.37: **Equivalent elastic surface beams OEB: Surface displacements**

The results again show the influence of the building weight adding to the magnitude of the surface displacements relative to the greenfield runs with the maximum displacement of 27.2mm (figures 8.37(a) and (c)) much greater than the maximum greenfield displacement of 16.9mm. The maximum settlement is very similar to the OMF run.

The settlement profile under the equivalent elastic beams is also flattened compared to the greenfield run OGF, due to the relative stiffness of the elastic beams with respect to the soil. For all stages, the elastic beams can been seen to tilt in response to the tunnelling, but do not exhibit any significant curvature.

The settlement profile can also be compared to that under the masonry facades in run OMF. The settlement under the beams for the front and rear walls (figures 8.37(a) and (b)) exhibits a flatter profile with less curvature than the settlement under the masonry facades (figures 8.34(a) and (b)). This is a similar observation to the symmetric analyses in section 8.2.4. In the oblique analyses, however, the difference between the masonry facades and the equivalent elastic beams in hogging is more clear with the elastic beams displaying negligible curvature in hogging (rear facade maximum Δ/L=0.0017%) compared to the masonry facades (rear facade maximum Δ/L=0.0269%) but exhibiting similar magnitude and settlement profiles in sagging.

The use of surface beams with equivalent elastic model properties gives very similar surface settlements to those under the full masonry facade for areas in sagging. The resulting surface displacements of the elastic beams in hogging sections however, despite closely matching magnitudes, exhibit negligible curvature under hogging conditions compared to the hogging exhibited by the masonry facades.

Influence of building stiffness

Analysis OEB was repeated with the in-plane bending stiffness for the beams varied by using five different multiples as shown in table 8.10. These factors were used to multiply the relevant in-plane bending stiffness properties for the beams given in tables 8.3 and 8.4.

Figure 8.38 shows the surface displacements for all beams after the final tunnelling stage.

As with the symmetric analyses, reducing the bending stiffness causes the profile to take a shape more like the greenfield profile, while the building weight acts to increase the magnitude of the displacements relative to the greenfield run. This is more evident in the rear facade (figure 8.38(b)) than the other walls

For the rear wall in hogging, it can be seen that the elastic beams with bending stiffness reduced to 1% of their original value (analysis OEB5 with $EI_{in}/100$) most closely replicate the surface profile under the masonry facades (OMF), giving an excellent match. This is interesting in the context of the requirement to choose and appropriate stiffness reduction factor f_b for the equivalent masonry beams as discussed in section 8.2.5 above. It is thus apparent that the appropriate factor is f_b=0.01. Further discussion of the choice of f_b for equivalent masonry beams is given below.

All elastic beam results give similar profiles for the front wall, with no significant deviation from the masonry facade profile. For each of the end walls, runs OEB5 and 6 can be seen to have the most similar displacement magnitude to the OMF run.

For sagging regions it can be seen that beams used in OEB with the original properties give a good match to the masonry facade settlement profile. The properties assigned to run OEB are thus considered to be appropriate for areas of sagging, however the in-plane bending stiffness needs to be reduced to a value of 1% of the original value to give a similar displacement profile in hogging.

8.3.5 Analysis with equivalent masonry surface beams

Surface displacement results from run OMB21 with the building represented by surface Timoshenko beams with the equivalent masonry beam model are presented in figures 8.39 to 8.41. The parameters of critical curvature and residual bending stiffness factor, used in the equivalent masonry beam model were κ_{crit}=1.0×10^{-5} and f_b=0.100 respectively. It was originally intended to use the same values as the symmetric central run (κ_{crit}=1.0×10^{-5} and f_b=0.010) but this was not possible due to computer hardware failures limiting the number of runs able to be performed.

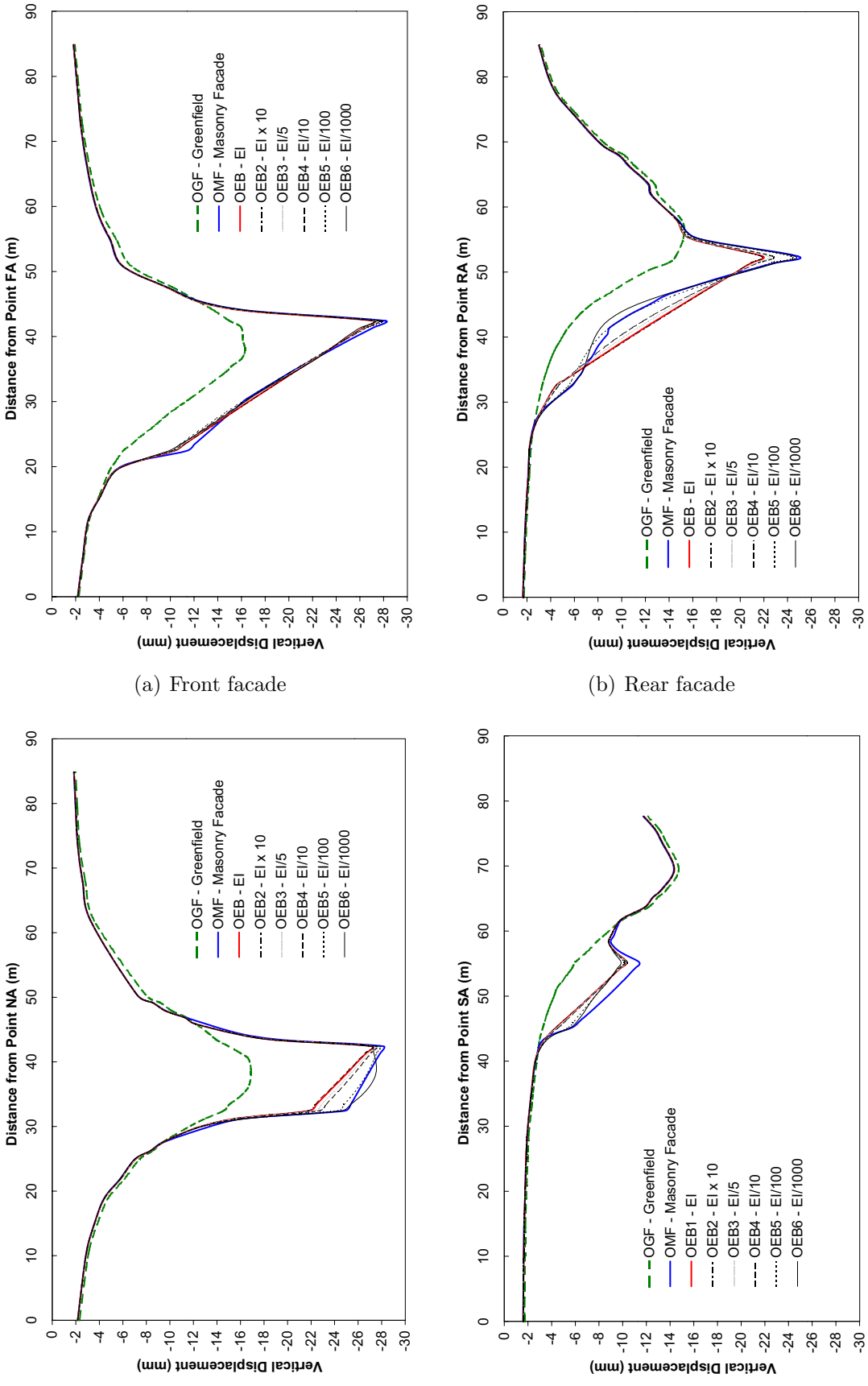

(a) Front facade

(b) Rear facade

(c) North end wall

(d) South end wall

Figure 8.38: **Equivalent elastic surface beams (Tunnelling Stage 8): Influence of bending stiffness**

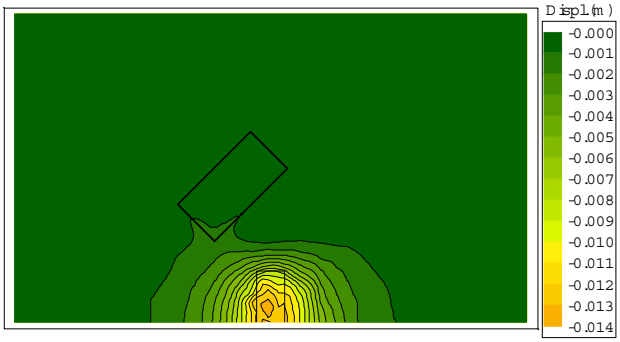

(a) Tunnelling Stage 1

(b) Tunnelling Stage 2

(c) Tunnelling Stage 3

(d) Tunnelling Stage 4

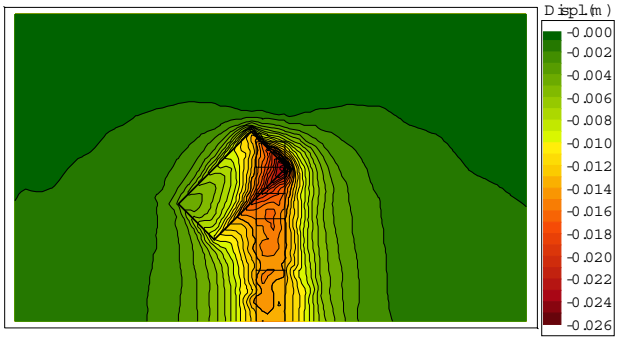

(e) Tunnelling Stage 5

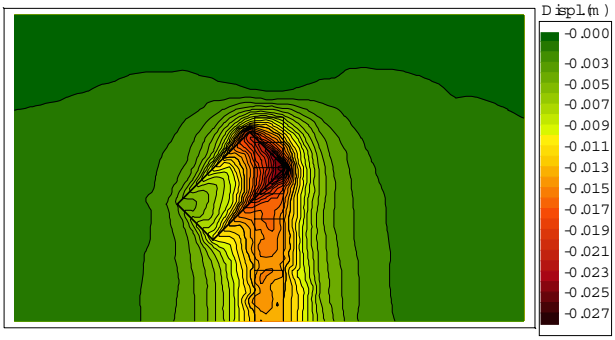

(f) Tunnelling Stage 6

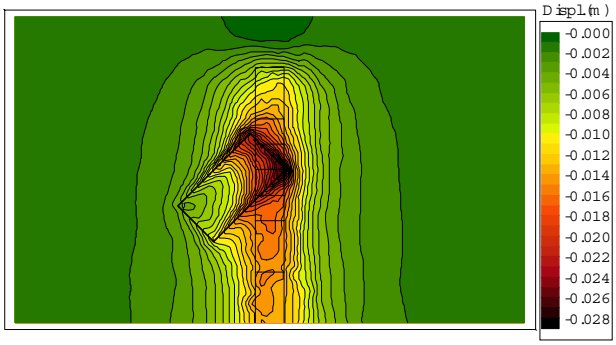

(g) Tunnelling Stage 7

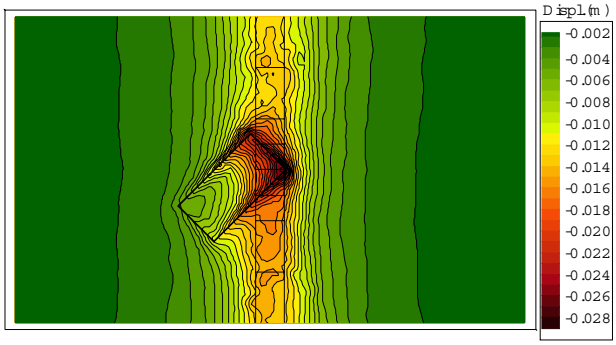

(h) Tunnelling Stage 8

Figure 8.39: **Equivalent masonry surface beams OMB: Surface displacement contours**

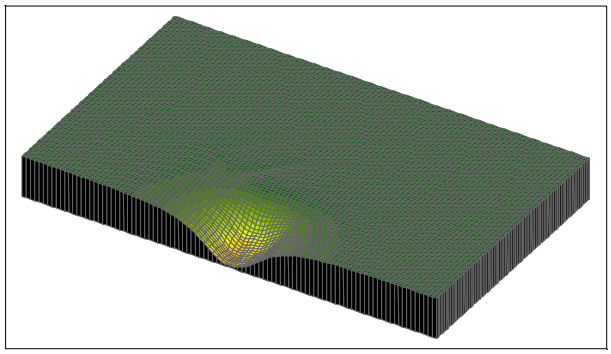

(a) Tunnelling Stage 1

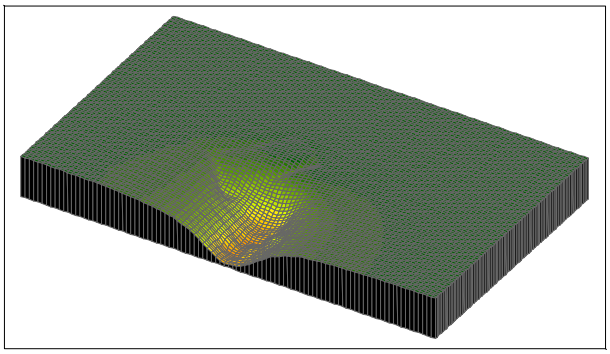

(b) Tunnelling Stage 2

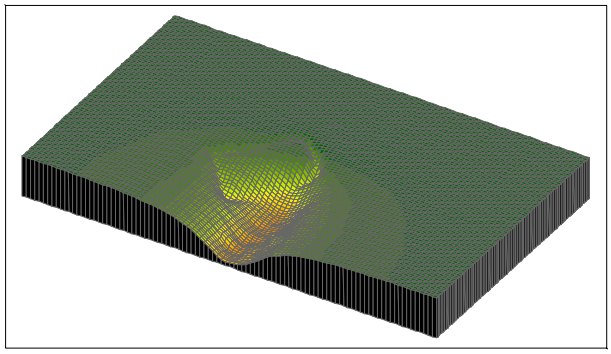

(c) Tunnelling Stage 3

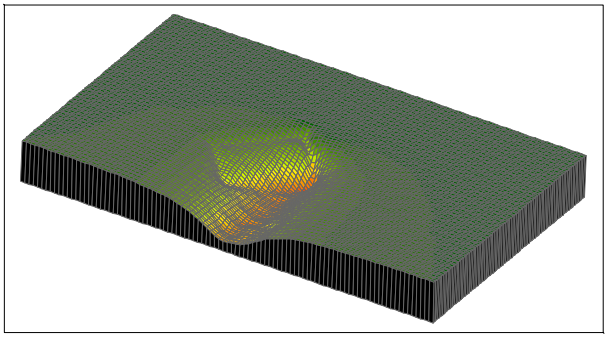

(d) Tunnelling Stage 4

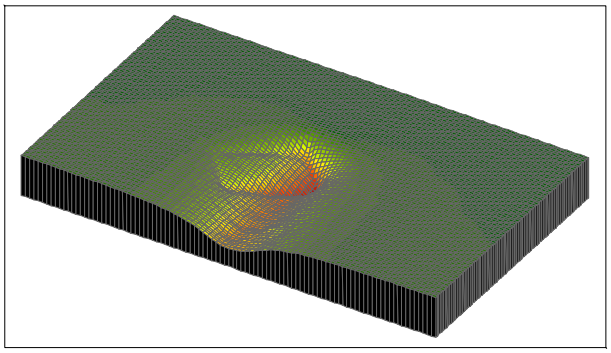

(e) Tunnelling Stage 5

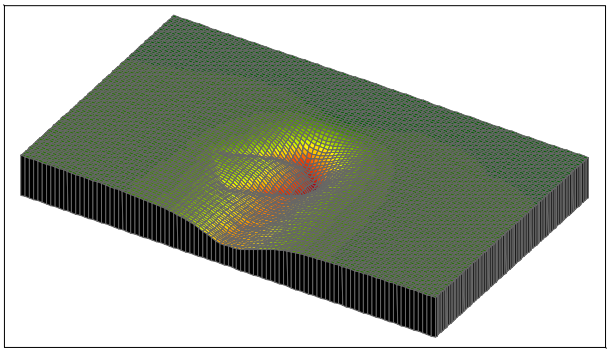

(f) Tunnelling Stage 6

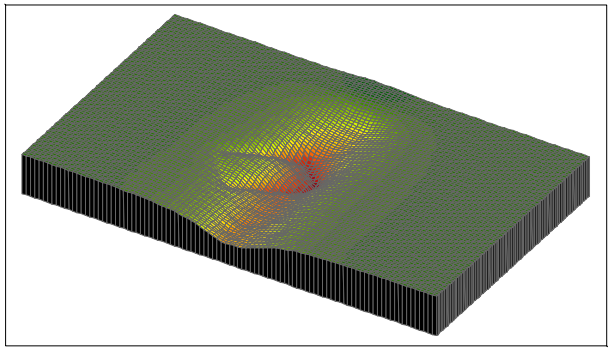

(g) Tunnelling Stage 7

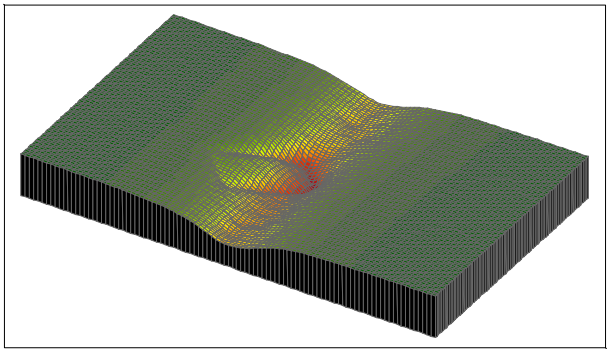

(h) Tunnelling Stage 8

Figure 8.40: **Equivalent masonry surface beams OMB: 3D Surface profile**

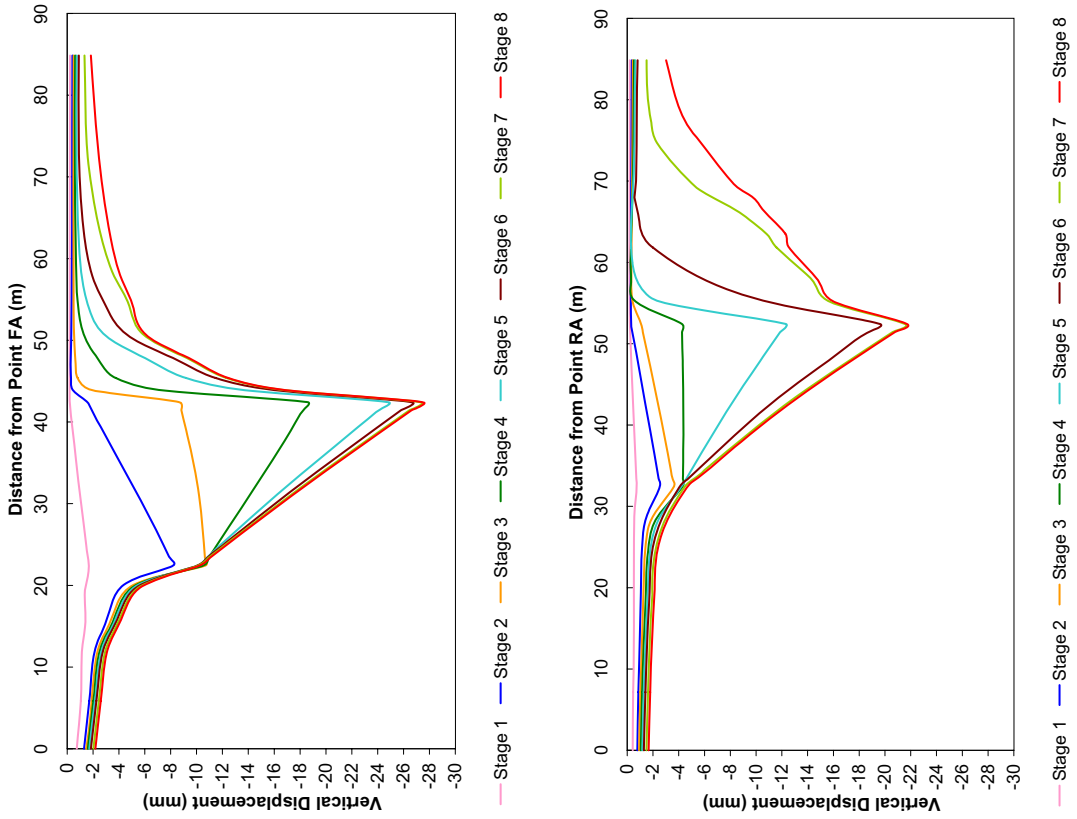

(a) Front facade

(b) Rear facade

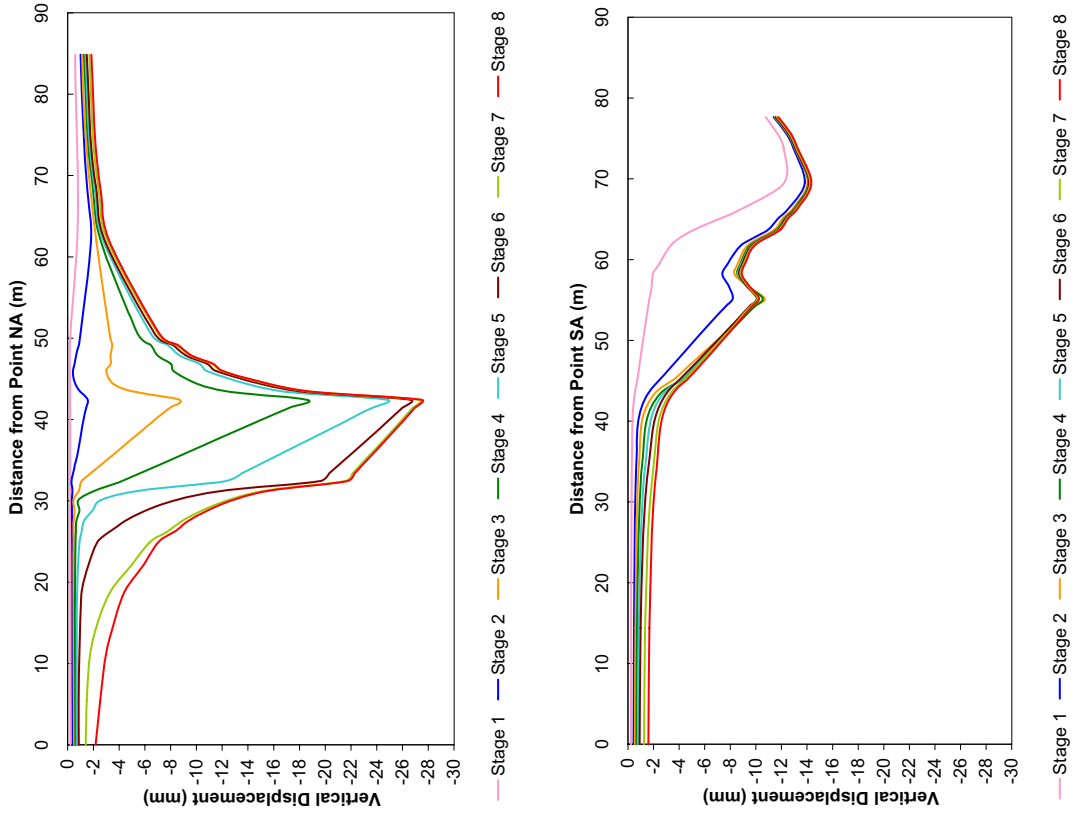

(c) North end wall

(d) South end wall

Figure 8.41: **Equivalent masonry surface beams OMB: Surface displacements**

Table 8.11: **Parameters for equivalent masonry beams - oblique analyses**

Analysis	κ_{crit}	f_b
OMB11	1.0×10^{-4}	0.100
OMB12	1.0×10^{-4}	0.010
OMB13	1.0×10^{-4}	0.001
OMB21	1.0×10^{-5}	0.100

The results again show the influence of the beams on the settlement profile and the additional vertical settlement due to the building weight. In areas where the beams are in sagging the settlement profile is the same as the OEB analysis described above. In areas of hogging, however, in particular the rear wall as shown in figure 8.41(b), there is greater hogging curvature (rear facade maximum Δ/L=0.0038%) than the response of run OEB (rear facade maximum Δ/L=0.0017%). This compares to the maximum hogging curvature of the masonry facade run with rear facade maximum Δ/L=0.0269%. Charts with comparisons including the OMF runs are given below.

Influence of κ_{crit} and f_b

The influence of the critical curvature, κ_{crit} and residual bending stiffness factor, f_b used in the equivalent masonry beam model is investigated in this section. Analysis type OMB was repeated using the range of different parameters shown in table 8.11. All other properties for the beams remained the same as those given in tables 8.3 and 8.4. The base analysis for which results are presented above is OMB21.

A discussion regarding choice of properties of f_b and κ_{crit} was given in section 8.2.5. From the oblique analyses described in this section it is apparent that the most appropriate value value for f_b is 0.01. The discussion in section 8.2.5 also indicated that κ_{crit} of 1.0×10^{-6} was potentially too low as the equivalent masonry beams lost stiffness at too low a hogging curvature. This indicates that the optimum combination of f_b and κ_c based on these results is f_b=0.01 and κ_{crit}=1.0×10^{-5}.

Section 8.2.5 also contains a discussion on the impact, in terms of requirement for different numbers of calculation steps, of the choice of f_b and κ_{crit}. As discussed above, limitations

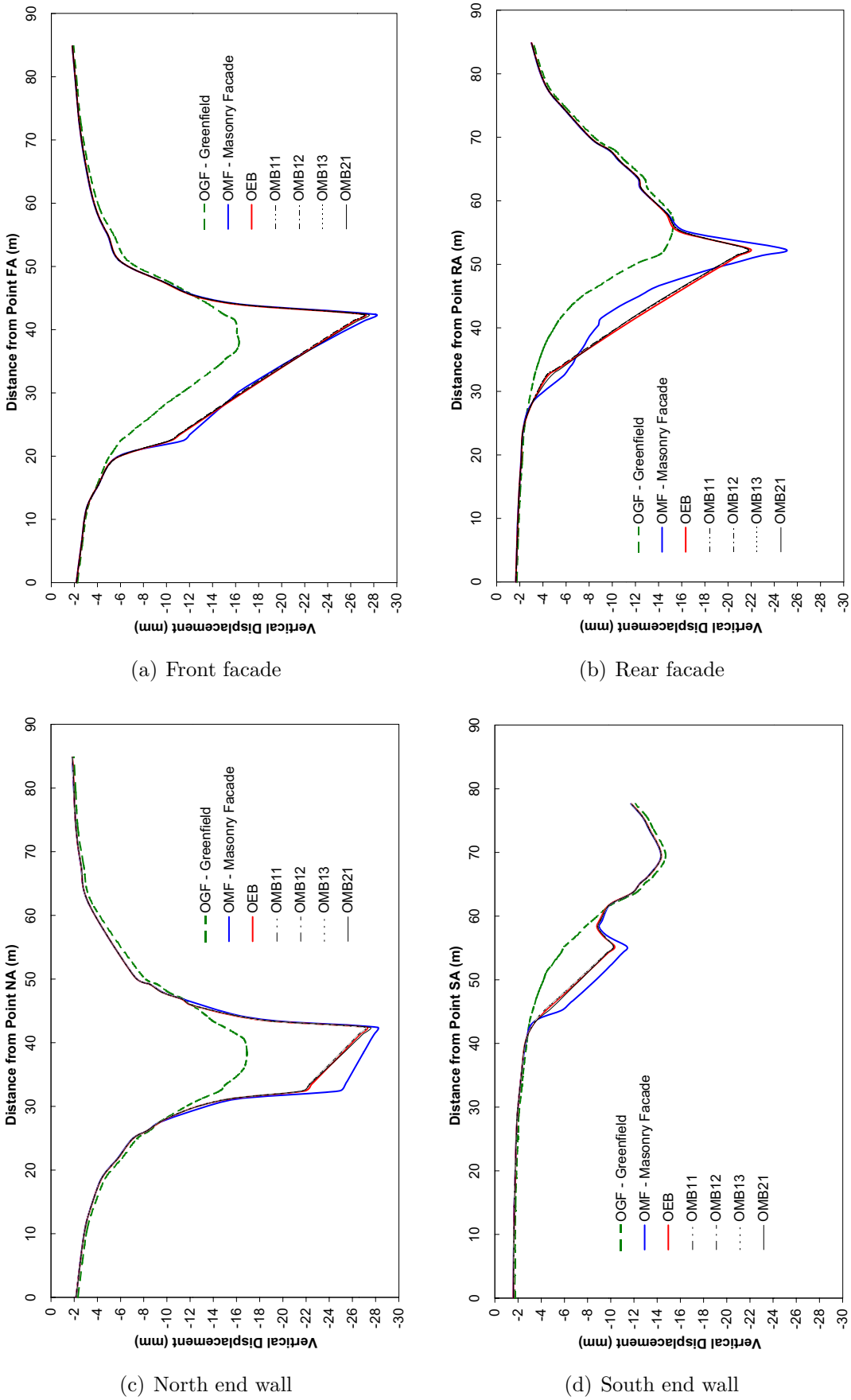

(a) Front facade

(b) Rear facade

(c) North end wall

(d) South end wall

Figure 8.42: **Equivalent masonry surface beams (Tunnelling Stage 8): Influence of κ_{crit} and f_b**

in the KONRAD hardware systems meant that it was not possible to obtain results for what would have been analyses OMB22 to OMB33 (in a similar fashion to the symmetric analyses). Repeated failures of the computing systems prevented the analysis of these models. It is recommended that these further analyses form part of future investigations.

The results in figure 8.42 show that varying f_b and κ_{crit} in the range shown has minimal effect on the displacement results with the OMB results generally plotting under the red OEB line. Run OMB21 can, however, be seen in figure 8.42(b) to hog more than the other runs, but not enough to replicate the response of the masonry facades.

8.3.6 Comparison of models

Numerical models

A clear comparison of each of the numerical models for the final tunnelling stage is given in figure 8.43. These charts show the main analyses without additional parametric results and are thus easier to compare. Discussion of the ability of the equivalent elastic and masonry beams to replicate the response of the masonry facades has been given in the preceding sections but figure 8.43 clearly shows the key conclusions. In sagging, the equivalent masonry surface beams replicate the response of the masonry facades very well, particularly for the front facade. In hogging, however, the masonry beams do not suffer the same relative displacement as the facades. This is further investigated using traditional response measures below.

Traditional assessment measures

Comparisons of the key responses of each of the masonry facade, elastic beam and masonry beam analyses from figure 8.43 are given using traditional building assessment parameters in table 8.12. The traditional assessment is undertaken using the methods described in section 2.5 including the Potts and Addenbrooke (1997) relative stiffness approach.

Following the approach of Augarde (1997) and Wisser (2002), the ground stiffness is given

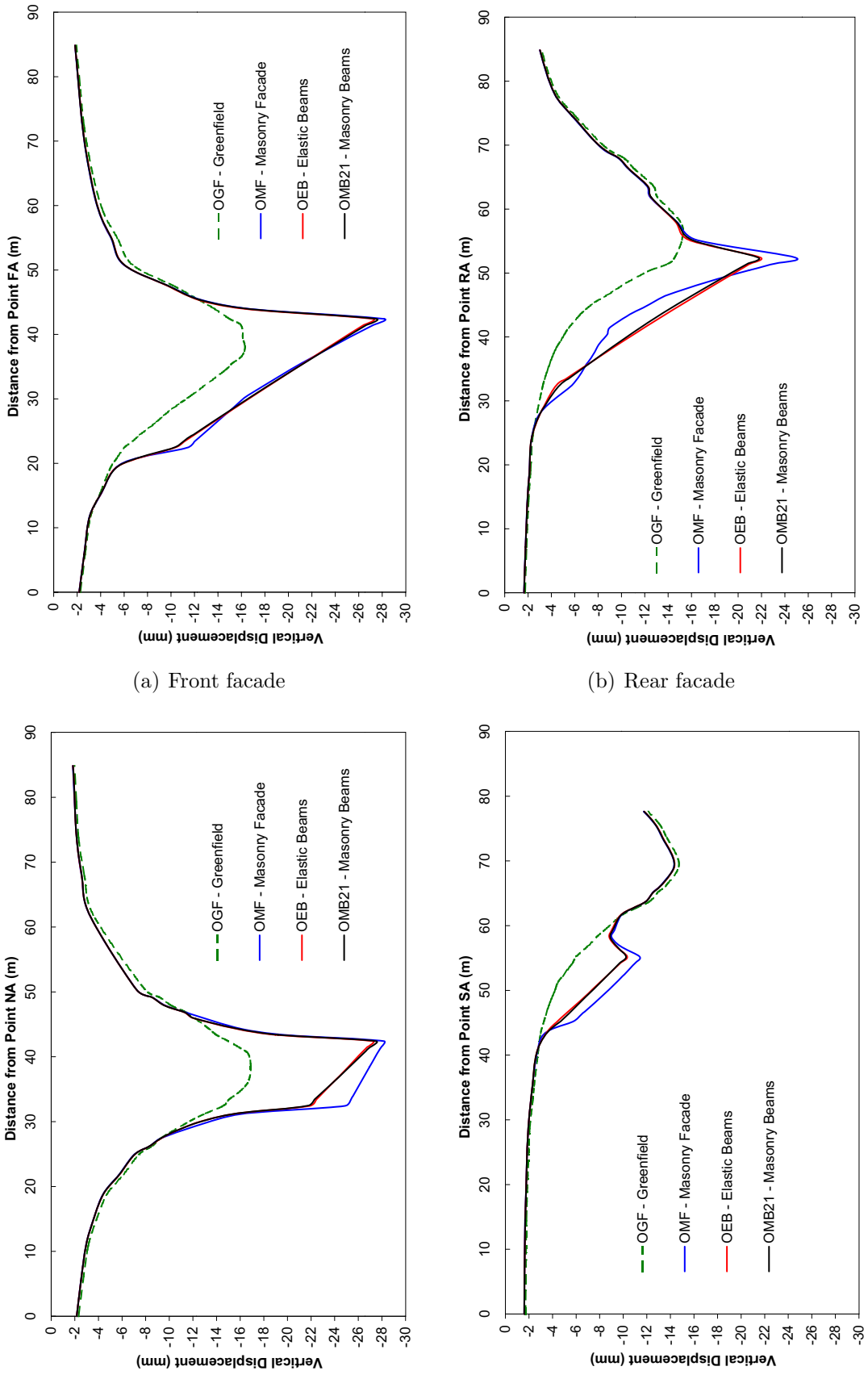

(a) Front facade

(b) Rear facade

(c) North end wall

(d) South end wall

Figure 8.43: **Oblique analyses: Comparison of numerical models**

a value of $E_s = 108 \times 10^3$kPa, which is 80% of the Young's modulus of the soil at a depth of $z/2$, where z is the depth to the tunnel centreline. For this analysis the bending and axial stiffness of the facades is calculated using the equivalent elastic approach of section 4.3. In hogging sections, the bending stiffness is reduced to 1% of the value in sagging reflecting the loss of stiffness in hogging as discussed in section 8.3.4. Note that this differs from the approach taken by Augarde (1997) and Wisser (2002) where the stiffness was reduced by 10%. If the stiffness is not reduced in hogging, the Potts and Addenbrooke (1997) relative stiffness method predicts a very rigid facade in hogging which is unrealistic.

Key features of the traditional approach are compared to similar results implied by the finite element analyses. In particular, the deflection ratio modification factors presented by Potts and Addenbrooke (1997) can be compared to those inferred from the displacement results from the finite element runs.

Key items of comparison from table 8.12 include that the finite element greenfield analysis gives less severe relative displacements and overall displacement magnitude than the traditional approach. For the rear facade, the different hogging response of the methods is clearly shown with the equivalent masonry beams hogging more than the elastic beams, but less than the masonry facades. The implied modification factor for the masonry beams is, however in excellent agreement with the factor from the Potts and Addenbrooke (1997) approach despite the magnitude of hogging being too low. For the front facade none of the finite element approaches exhibited any sagging leading to implied modification factors of 0.0 in this mode. In hogging, the masonry facades and beams exhibited greater relative hogging displacement than the greenfield analysis leading to implied modification factors greater than 1.0. This indicates the relative susceptibility of masonry facades to hogging displacements. Differences between the traditional and finite element approaches are thought to result from the fact that the traditional approach involves projecting the building onto the transverse settlement trough, whereas for the finite element results, displacement profiles were taken exactly under the facade alignment. The fact that the greenfield finite element profile is shallower and wider than the Gaussian profile is also a differentiating factor.

Table 8.12: **Oblique Analyses: Traditional Assessment and Finite Element Model Comparison**

REAR FACADE					
Data	**Traditional**	**OGF**	**OMF**	**OEB**	**OMB**
Greenfield (prior to considering building)					
Max Settlement (mm)	31.3	16.9	-	-	-
Max Δ/L Hog (DR^g_{hog}%)	0.0579	0.0136	-	-	-
Max Δ/L Sag (DR^g_{sag}%)	0.0025	0.0229	-	-	-
Potts and Addenbrooke (1997) modification factors					
$M^{DR_{hog}}$	0.2	-	-	-	-
$M^{DR_{sag}}$	0.1	-	-	-	-
Modified traditional					
Max Δ/L Hog (DR_{hog}%)	0.0116	-	-	-	-
Max Δ/L Sag (DR_{sag}%)	0.0003	-	-	-	-
Finite element results with building					
Max Settlement (mm)	-	-	24.9	21.9	21.7
Max Δ/L Hog (%)	-	-	0.0269	0.0017	0.0038
Max Δ/L Sag (%)	-	-	N/A	N/A	N/A
Implied modification factors from finite element results					
Implied $M^{DR_{hog}}$	-	-	1.97	0.13	0.28
Implied $M^{DR_{sag}}$	-	-	N/A	N/A	N/A
FRONT FACADE					
Data	**Traditional**	**OGF**	**OMF**	**OEB**	**OMB**
Greenfield (prior to considering building)					
Max Settlement (mm)	31.3	16.9	-	-	-
Max Δ/L Hog (DR^g_{hog}%)	0.0362	0.0018	-	-	-
Max Δ/L Sag (DR^g_{sag}%)	0.1047	0.0188	-	-	-
Potts and Addenbrooke (1997) modification factors					
$M^{DR_{hog}}$	0.2	-	-	-	-
$M^{DR_{sag}}$	0.1	-	-	-	-
Modified traditional					
Max Δ/L Hog (DR_{hog}%)	0.0072	-	-	-	-
Max Δ/L Sag (DR_{sag}%)	0.0105	-	-	-	-
Finite element results					
Max Settlement (mm)	-	-	28.2	27.2	27.5
Max Δ/L Hog (%)	-	-	0.0082	0.0006	0.0013
Max Δ/L Sag (%)	-	-	N/A	N/A	N/A
Implied modification factors from finite element results					
Implied $M^{DR_{hog}}$	-	-	4.53	0.31	0.71
Implied $M^{DR_{sag}}$	-	-	0.00	0.00	0.00

8.3.7 Summary

The comparison of the response of equivalent elastic and masonry beams to that of masonry facades in analyses of tunnelling under a building oblique to the centreline results in the following key points.

The response of the equivalent elastic beams shows good agreement with the profile of the masonry facades for sagging regions. In hogging regions, however, the EEBs are too stiff. Analyses of EEBs with a range of reduced in-plane bending stiffnesses leads to the conclusion that a reduction in bending stiffness to 1% of the original value is required to match most closely the response of the masonry facades in hogging.

The equivalent masonry beams respond in a similar fashion to the elastic beams in sagging as expected. In hogging regions with the parameters investigated, the beams can be seen to lose stiffness and hog more than the elastic beams, but not to the degree necessary to replicate exactly the masonry facade response. More combinations of suitably low values of critical curvature (κ_{crit}) and residual bending stiffness (f_b) should be investigated as part of future work in order to improve the response of the equivalent masonry beams.

8.4 Conclusion

The numerical models of building response to tunnelling presented in this chapter were undertaken to evaluate the three-dimensional surface beam approach for modelling masonry buildings developed in earlier chapters of this thesis. In particular, to assess the use of 3D Timoshenko beam elements and the equivalent elastic and equivalent masonry beam models to replicate masonry buildings by comparison with finite element analyses. The discussion and summaries presented in this chapter lead to a number of conclusions in this respect.

It is apparent that the stiffness of surface beams representing masonry facades in sagging should be determined by using the procedures accounting for the openings and geometry of the individual facades developed in this thesis. It is also clear that a reduction of the in-plane bending stiffness for surface beams in hogging is required to reflect properly

the response of masonry facades. Beams with properties in sagging as described by the equivalent elastic beam method method are thus recommended, but in hogging the in-plane bending stiffness should be reduced by a residual stiffness factor, f_b=0.01.

The rate at which the equivalent masonry beams lose their stiffness is governed by the critical curvature. The most appropriate value of the critical curvature, is recommended as κ_{crit}=1.0×10^{-5}. This recommendation is made subject to the requirement for further investigation of the parameters f_b and κ_{crit} in analyses involving different amounts of hogging curvature.

Overall, the use of equivalent masonry beams to model masonry facades in tunnelling analyses using the methods developed in this thesis has been shown to be a useful and successful alternative to modelling the full building in a finite element analysis.

Numerical modelling of masonry building response to tunnelling using equivalent masonry beams with properties as determined in this chapter will be evaluated by comparison to tunnelling case studies in Chapter 9.